

# Synthesis, Chemical, and Thermoelectric Properties of n-Type $\pi$ -Conjugated Polymer Composed of 1,2,4-Triazole and Pyridine Rings and Its Metal Complexes

Isao Yamaguchi, Tomoyuki Nagano

Department of Chemistry, Interdisciplinary Graduate School of Science and Engineering, Shimane University, 1060 Nishikawatsu, Matsue 690-8504, Japan

Correspondence to: I. Yamaguchi (E-mail: iyamaguchi@riko.shimane-u.ac.jp)

**ABSTRACT:** A soluble n-type  $\pi$ -conjugated polymer (**polymer 1**) composed of a 1,2,4-triazole ring substituted by a 4-*n*-octylphenyl subunit at the 4-position of the 1,2,4-triazole ring and pyridine-2,5-diyl rings was synthesized by Ni(cod)<sub>2</sub> (cod = 1,5-cyclooctadiene) promoted dehalogenation polycondensation of 3,5-bis(2-bromopyridyl)-4-*n*-octylphenyl-1,2,4-triazole (**monomer 1**). A polymer complex (**polymer-BiCl<sub>3</sub>**) was synthesized by the reaction of **polymer 1** with BiCl<sub>3</sub>. The UV-vis spectrum of **polymer 1** exhibited an absorption maximum ( $\lambda_{\text{max}}$  value) at a longer wavelength than that exhibited by **monomer 1** revealing that its  $\pi$ -conjugation system was expanded along the polymer chain. **Polymer 1** was electrochemically active in film, and the electrochemical reaction was accompanied with electrochromism. Thermoelectric properties of **polymer 1** and **polymer-BiCl<sub>3</sub>** were investigated. © 2013 Wiley Periodicals, Inc. *J. Appl. Polym. Sci.* **2014**, *131*, 39928.

**KEYWORDS:** conducting polymers; thermal properties; electrochemistry

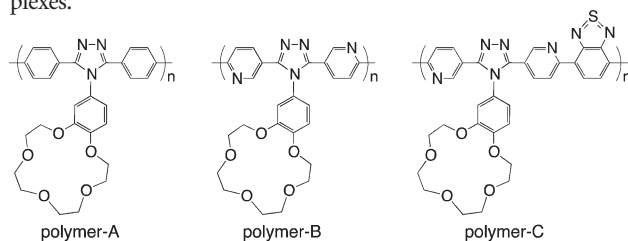
Received 8 June 2013; accepted 21 August 2013

DOI: 10.1002/app.39928

## INTRODUCTION

$\pi$ -Conjugated polymers have attracted considerable attention due to their interesting chemical properties and practical applications because they can undergo a reductive (n-type) or an oxidative (p-type) doping that effectively converts them into conducting materials.<sup>1</sup> However, reports on n-type conductive polymers are considerably less than those on p-type ones because of the difficulty associated with synthesizing n-type  $\pi$ -conjugated polymers and their low solubility in organic solvents.<sup>2-12</sup> Recently, we reported n-type  $\pi$ -conjugated polymers with a benzo-15-crown 5-ether (benzo15C5) subunit substituted at the 4-position of a 1,2,4-triazole ring, as shown below.<sup>13,14</sup> These polymers exhibited a stable n-doping state compared with polymers with the 4-methoxyphenyl group instead of the benzo15C5 subunit. The stability of the n-doping state in the polymers is attributed to the fact that a dopant cation (Na<sup>+</sup>) was captured in the crown ether (CE) subunit of the polymers during n-doping. However, the low solubilities of the polymers in organic solvents restricted investigation of their specific optical properties in solution. In this study, a  $\pi$ -conjugated polymer (**polymer 1**) composed of a 1,2,4-triazole ring substituted by a 4-*n*-octylphenyl subunit at the 4-position of the 1,2,4-triazole ring and pyridine-2,5-diyl rings was synthesized by Ni(cod)<sub>2</sub> promoted dehalogenation polycondensation of 3,5-bis(2-bromopyridyl)-4-*n*-hexylphenyl-1,2,4-triazole

(**monomer 1**). The *n*-octyl group in the polymer could improve solubility of the polymer in organic solvents, and the pyridine rings in the polymer enables the synthesis of polymer metal complexes.



Thermoelectric materials have attracted significant attention as simple, automatic, and ecofriendly means of energy conversion owing to their unique capability to directly convert heat to electricity.<sup>15,16</sup> Characteristics such as weight, size, and flexibility are important considerations for the preparation of thermoelectric devices. These are inherent advantages of polymer thermoelectric materials as compared with inorganic thermoelectric materials. Bi<sub>2</sub>Te<sub>3</sub> is one of the most studied thermoelectric materials, because it exhibits a high Seebeck coefficient and electric conductivity. Polymer composites consisting of p-type  $\pi$ -conjugated polymers such as polyethylenedioxythiophene and polyhexylthiophene and Bi<sub>2</sub>Te<sub>3</sub> were prepared to combine the merits of polymers, such as weight, size, and flexibility, and the good

thermoelectric performance of  $\text{Bi}_2\text{Te}_3$ .<sup>17,18</sup> The thermoelectric properties of these composites were investigated. For the preparation of thermoelectric devices, both p- and n-type conductors are required. However, there are limited studies of the thermoelectric properties of n-type conjugated polymers. In this study, we investigated the thermoelectric properties of **polymer 1** and its complex with  $\text{BiCl}_3$ . The complex was synthesized by metal coordination with pyridine rings in **polymer 1**. This polymer complex could be a useful precursor for the synthesis of  $\pi$ -conjugated polymer- $\text{Bi}_2\text{Te}_3$  complexes.  $\text{Bi}_2\text{Te}_3$  is synthesized by the reaction of bismuth chloride and sodium telluride in the presence of amines.<sup>18</sup> To the best of our knowledge, this is the first report of the thermoelectric properties of an n-type conjugated polymer-metal complex.

Herein, we report the synthesis of a n-type  $\pi$ -conjugated polymer comprising  $\pi$ -electron deficient aromatic rings and its  $\text{BiCl}_3$  complex, along with their optical, electrochemical, electric, and thermoelectric properties. In addition, the optical properties of **polymer 1** solution in the absence and presence of metal salts are also reported.

## EXPERIMENTAL

### General

Solvents were dried, distilled, and stored under nitrogen. *N,N'*-Bis[chloro(*p*-bromopyridyl)methylene]hydrazine was synthesized according to the reported manner.<sup>19,20</sup> Other reagents were purchased and used without further purification. Reactions were carried out with standard Schlenk techniques under nitrogen.

Infrared (IR) and nuclear magnetic resonance (NMR) spectra were recorded on a JASCO FT/IR-660 PLUS spectrophotometer with a KBr pellet and JEOL AL-400 and JEOL ECX-500 spectrometers, respectively. Elemental analysis was conducted on a Yanagimoto MT-5 CHN corder. GPC analyses were carried out by a Jasco 830 refractometer with polystyrene gel columns (K-803 and K-804) using chloroform as an eluent with a refraction index detector. Matrix-assisted laser desorption ionization time-of-light mass spectroscopy (MALDI TOF-MS) measurement was carried with a JEOL JMS-S3000. *trans*-2-[3-(4-*tert*-Butylphenyl)-2-methyl-2-propenylidene]malononitrile was used as a matrix. Ultraviolet-visible (UV-vis) and photoluminescence (PL) spectra were obtained by a JASCO V-560 spectrometer and a JASCO FP-6200, respectively. Quantum yields were calculated by using a diluted ethanol solution of 7-dimethylamino-4-methylcoumarin as the standard. Cyclic voltammetry was performed with a Hokuto Denko HSV-110. Pt plate (1 cm × 1 cm) and wire were used as the working and reference electrodes, respectively. A sample film was prepared by cast of the chloroform solution of the sample on a Pt electrode, followed by remove of the solvent under vacuum. Electric conductivity measurement was conducted by an Advantest R8340A ultra high resistance meter with a two-probe method.

### Synthesis of Monomer 1

*N,N'*-Bis[chloro(*p*-bromopyridyl)methylene]hydrazine (1.6 g, 3.8 mmol) and 4-*n*-octylaniline (1.2 g, 5.8 mmol) were dissolved in 15 mL of *N,N*-dimethylaniline under  $\text{N}_2$ . After the solution was stirred at 135°C for 30 h, the reaction solution was cooled to

room temperature and added to a mixture of chloroform (100 mL) and water (100 mL). The organic layer was dried over sodium sulfate and evaporated under vacuum. The solvent was removed under vacuum and resulting solid was reprecipitated from hexane and then recrystallized from a solution of chloroform and ethanol ( $v/v = 1/1$ ). **Monomer 1** was collected by filtration, dried under vacuum, and obtained as a white crystal (0.89 g, 42%). <sup>1</sup>H-NMR (400 MHz,  $\text{CDCl}_3$ ):  $\delta$  8.33 (d,  $J = 2.4$  Hz, 2H), 7.87 (dd,  $J = 2.0$  and 6.4 Hz, 2H), 7.13–34 (m, 4H), 7.12 (d,  $J = 8.4$  Hz, 2H), 2.69 (t,  $J = 1.6$  Hz, 2H), 1.66 (s, 2H), 1.32 (m, 10H), 0.90 (t,  $J = 6.8$  Hz, 3H). <sup>13</sup>C-NMR (125 MHz,  $\text{CDCl}_3$ ):  $\delta$  152.9, 152.2, 148.6, 146.7, 138.4, 131.3, 130.8, 127.2, 124.4, 122.0, 35.6, 31.9, 31.0, 30.9, 29.4, 29.2, 22.7, 14.1. Calcd. for  $\text{C}_{26}\text{H}_{27}\text{Br}_2\text{N}_5$ : C, 54.85; H, 4.78; N, 12.30. Found: C, 54.60; H, 4.91; N, 12.12.

### Synthesis of Polymer 1

$\text{Ni}(\text{cod})_2$  (0.34 g, 1.2 mmol) and 2,2-bipyridyl (0.20 g, 1.3 mmol), cod (0.13 g, 1.2 mmol) were dissolved in 10 mL of dry DMF under nitrogen. To the solution was added a DMF solution (5 mL) of **monomer 1** (0.57 g, 1.0 mmol) at 60°C. The reaction solution was stirred at 85°C for 72 h. The precipitate was collected by filtration, washed with an aqueous solution of ammonia (three times), an aqueous solution of ethylenediaminetetraacetic acid, and methanol, and dried under vacuum to give **polymer 1** as a yellow powder (0.26 g, 62%). <sup>1</sup>H-NMR (400 MHz,  $\text{CDCl}_3$ ):  $\delta$  8.70 (2H), 8.24 (2H), 7.79 (2H), 7.08–7.24 (4H), 2.61 (2H), 1.22 (12H), 0.81 (3H). <sup>13</sup>C-NMR (125 MHz,  $\text{CDCl}_3$ ):  $\delta$  155.6, 153.2, 153.0, 150.6, 149.2, 148.5, 137.9, 136.1, 126.9, 124.3, 123.1, 120.5, 113.6, 112.6, 71.2, 70.4, 69.3, 69.1, 68.8. Calcd for  $(\text{C}_{26}\text{H}_{27}\text{N}_5 \cdot 0.3\text{H}_2\text{O})_n$ : C, 75.26; H, 6.70; N, 16.88. Found: C, 75.40; H, 6.23; N, 16.66.

### Synthesis of Polymer-BiCl<sub>3</sub>

A chloroform solution (10 mL) of **polymer 1** (0.10 g, 0.25 mmol) and  $\text{BiCl}_3$  (78 mg, 0.25 mmol) was stirred at 20°C for 12 h. The resulting precipitate was collected by filtration, washed with acetone, and dried under vacuum to give **polymer-BiCl<sub>3</sub>** as a yellow solid (0.11 g). Calcd for  $(\text{C}_{26}\text{H}_{27}\text{N}_5 \cdot 0.36\text{BiCl}_3)_n$ : C, 59.65; H, 5.16; N, 13.40. Found: C, 59.65; H, 5.00; N, 13.49.

### Electric Conductivity and Seebeck Coefficient Measurements

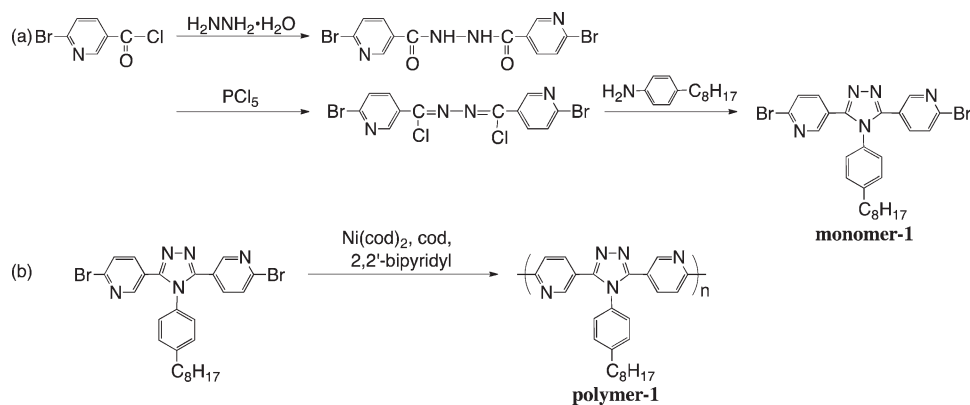
Electrical conductivity was measured by the standard two-probe method using an Advantest R8340A ultra high resistance meter. The n-doping was carried out by using sodium naphthalenide according to the usual manner.<sup>11</sup>

The Seebeck coefficient was obtained by measuring the electrical potential difference when a temperature gradient was established between two ends of the molded pellet. The Seebeck coefficient of Ni at 300 K was measured as a reference sample, and the measured value of  $-19 \mu\text{V K}^{-1}$  was in good agreement with the literature value of  $-19.24 \mu\text{V K}^{-1}$ .

## RESULTS AND DISCUSSION

### Synthesis

A monomer with a 3,5-bis(2-bromopyridyl)-1,2,4-triazole ring substituted by 4-*n*-octylphenyl group (**monomer 1**) was synthesized through the 2 : 1 reaction of 4-bromopicolinic acid



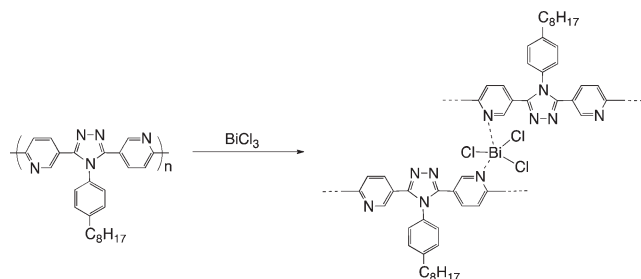
Scheme 1. Synthesis of monomer and polymer.

chloride with hydrazine monohydrate and the following ring-closure reaction with 4-*n*-octylaniline (Scheme 1a).

Dehalogenation polycondensation of **monomer 1** carried out using Ni(cod)<sub>2</sub> as a condensation reagent afforded **polymer 1** in 62% yield (Scheme 1b). Reaction of **polymer 1** and trichlorobithmuth afforded **polymer-BiCl<sub>3</sub>** (Scheme 2). A possible structure of **polymer-BiCl<sub>3</sub>** is shown in Scheme 2.

**Polymer 1** was soluble in chloroform and trifluoroacetic acid at room temperature, but was insoluble in polar organic solvents such as *N,N*-dimethylformamide (DMF) and dimethyl sulfoxide (DMSO). This solubility is contrast to that of polymer A, polymer B, and polymer C, which are partly soluble in DMF and DMSO and insoluble in chloroform. The improved solubility of **polymer 1** in chloroform is attributed to the presence of the octyl group in the polymer. On the other hand, **polymer-BiCl<sub>3</sub>** was soluble in acidic solvents such as sulfuric acid and trifluoroacetic acid, but was insoluble in organic solvents. The low solubility of **polymer-BiCl<sub>3</sub>** in organic solvents is probably due to its crosslinked structure shown in Scheme 2. It has been reported that BiCl<sub>3</sub> can coordinate from one to three pyridine molecules.<sup>21</sup> Elemental analysis suggested that **polymer-BiCl<sub>3</sub>** contained 0.36 molecule of BiCl<sub>3</sub> per polymer repeating unit.

The  $M_n$  and  $M_w$  values of **polymer 1**, determined by GPC measurement, are 3400 and 4330, respectively. The molecular weights of **polymer-BiCl<sub>3</sub>** could not be determined because of its insolubility in the eluent. The MALDI TOF-MS measurement suggested that the  $m/z$  range of **polymer 1** was from 1779 to 4740.

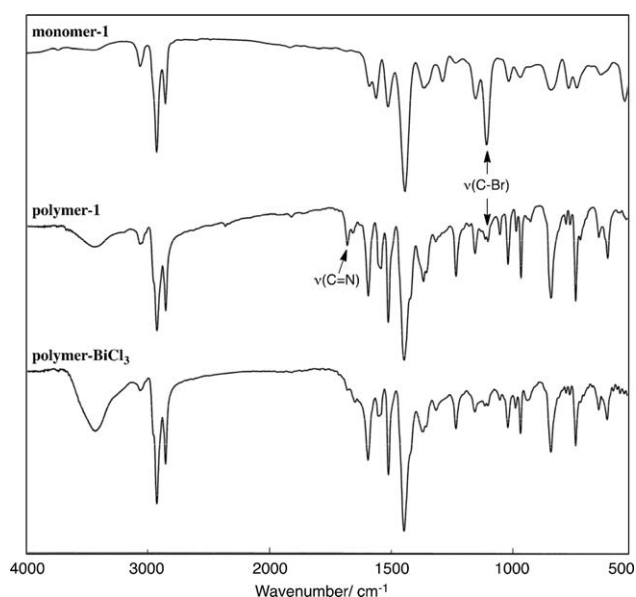


Scheme 2. Synthesis of polymer complex.

### IR and <sup>1</sup>H-NMR Spectra

Figure 1 shows the IR spectra of **monomer 1**, **polymer 1**, and **polymer-BiCl<sub>3</sub>**. The peak corresponding to the stretching vibrations of a C-Br bond is observed at 1049 cm<sup>-1</sup> in the IR spectrum of **monomer 1**, whereas it decreased in the IR spectra of **polymer 1**. The decrement suggests that the expected polycondensations occurred. The peak corresponding to the stretching vibrations of a C=N of **polymer 1** is observed at 1681 cm<sup>-1</sup>. This peak decreases in the IR spectrum of **polymer-BiCl<sub>3</sub>**, suggesting that the metal complexation occurred at the pyridine rings of **polymer 1**. The strong peaks corresponding to the octyl group are observed at 2853 and 2924 cm<sup>-1</sup> in the IR spectra of **monomer 1**, **polymer 1**, and **polymer-BiCl<sub>3</sub>**. The appearance of the absorption corresponding to ν(O-H) around 3500 cm<sup>-1</sup> in the IR spectra of the polymers suggests that they contain hydrated water molecule(s). This view is consistent with the analytical data.

Figure 2 shows the <sup>1</sup>H-NMR spectra of **monomer 1** and **polymer 1** in CDCl<sub>3</sub>. The peak assignments are indicated in the figure. The signals corresponding to the aromatic (H<sup>a</sup>~H<sup>e</sup>) and

Figure 1. IR spectra of **monomer 1**, **polymer 1**, and **polymer-BiCl<sub>3</sub>**.

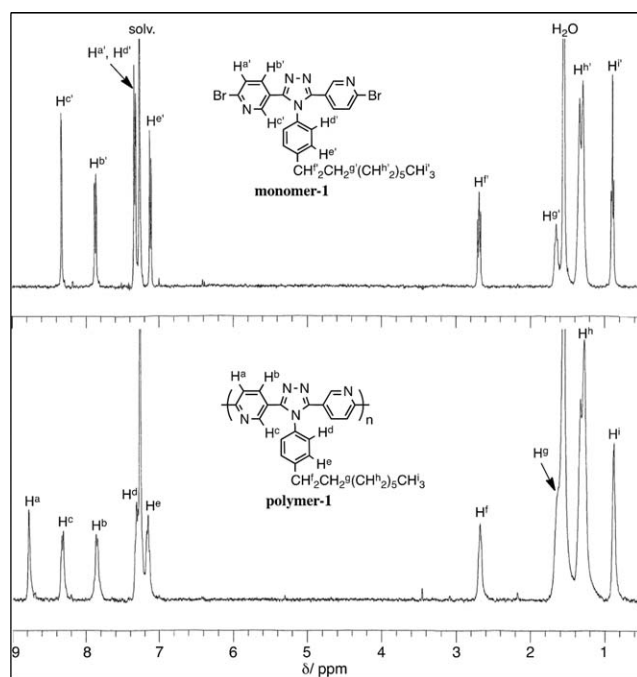


Figure 2.  $^1\text{H-NMR}$  spectra of **monomer 1** and **polymer 1** in  $\text{CDCl}_3$ .

octyl ( $\text{H}^f \sim \text{H}^i$ ) protons of **polymer 1** are observed in the ranges  $\delta$  7.32–8.76 and  $\delta$  0.88–2.68, respectively. The relative peak integral ratio supports the structure shown in Scheme 1b. The peaks corresponding to the pyridine protons ( $\text{H}^a$ ,  $\text{H}^b$ , and  $\text{H}^c$ ) of **polymer 1** shifted to lower magnetic field positions as compared with those of **monomer 1**. The degree of the down field shift is the largest in the peak corresponding to  $\text{H}^a$ . These shifts are attributed to the replacement of the bromo group with the electron-withdrawing pyridine ring in the polymer.

#### UV–Vis and Photoluminescence Spectra

Optical data of **monomer 1**, **polymer 1**, and the polymer chloroform solution in the presence of excess amount of metal salts are summarized in Table I. Figure 3 shows the UV–vis spectra of the chloroform solution of **polymer 1** in the absence and presence of an excess amount of metal salts.

The absorption maximum ( $\lambda_{\text{max}} = 343 \text{ nm}$ ) of **polymer 1** was longer than that of **monomer 1** ( $\lambda_{\text{max}} = 285 \text{ nm}$ ), suggesting that the  $\pi$ -conjugation system was expanded along the polymer chain. As shown in Figure 3, the UV–vis spectrum of the **polymer 1** solution was mostly unchanged after the addition of LiBr. However, after the addition of  $\text{Zn}(\text{OAc})_2$  and  $\text{AgNO}_3$ , the  $\lambda_{\text{max}}$  value of the **polymer 1** solution red-shifted by 9 nm and blue-shifted by 21 nm, respectively. The bathochromic shift of **polymer 1**, after the addition of  $\text{Zn}(\text{OAc})_2$ , was caused by the formation of a regular tetrahedral complex between  $\text{Zn}^{2+}$  and two neighboring pyridine rings in **polymer 1**, as shown in Chart 1a. This metal complexation causes the crosslinking of the polymer chain and improves coplanarity. It is well known that  $\text{Zn}(\text{II})$  salts typically form regular tetrahedral complexes with bidentate ligands.

The hypsochromic shift of **polymer 1**, after the addition of  $\text{AgNO}_3$ , was caused by the formation of the linear complex

Table I.  $\lambda_{\text{max}}$  and  $\lambda_{\text{em}}$  Values of the Chloroform Solution of **Polymer 1** in the Absence and Presence of Metal Salts

	None	LiBr	$\text{Zn}(\text{OAc})_2$	$\text{AgNO}_3$
$\lambda_{\text{max}}$ (nm)	343	342	352	322
$\lambda_{\text{em}}$ (nm)	395, 410	394, 409	411, 435	Quenched

between  $\text{Ag}^+$  and two pyridine groups in **polymer 1**, as shown in Chart 1b. However, in this case, metal complexation causes the crosslinking of the polymer chain but does not improve the coplanarity. It is well known that  $\text{Ag}(\text{I})$  salts form linear type metal complexes with monodentate ligands. In addition, the UV–vis spectrum of polymer A did not exhibit bathochromic and hypsochromic shifts after the addition of  $\text{Zn}(\text{OAc})_2$  and  $\text{AgNO}_3$ . This further supports the assumed formation of the complex between the metal salts and the pyridine rings in **polymer 1**.

**Monomer 1** and **polymer 1** were photoluminescent in chloroform. Figure 4 shows the PL spectra of the chloroform solution of **polymer 1** in the absence and presence of metal salts. The emission peak position of **polymer 1** was longer than that of **monomer 1** ( $\lambda_{\text{em}} = 349$  and  $359 \text{ nm}$ ) in chloroform. This observation is consistent with the result that the  $\lambda_{\text{max}}$  value of **polymer 1** was larger than that of **monomer 1**. The PL peak of the polymer appears at the onset position of its absorption band, as usually observed with photoluminescent aromatic compounds. The PL peak intensity of **polymer 1** in chloroform decreased with a bathochromic shift of 25 nm after the addition of  $\text{Zn}(\text{OAc})_2$  to the solution. The bathochromic shift of the PL peak corresponds to the observation that the chloroform solution of **polymer 1** caused a bathochromic shift by the addition of  $\text{Zn}(\text{OAc})_2$  to the solution. The addition of  $\text{AgNO}_3$  to the solution led to the quenching of the PL of **polymer 1** in chloroform. The quenching and decrease in the PL are attributed to the formation of polymer complexes between the metal salts and polymer chains. This attribution is consistent with a

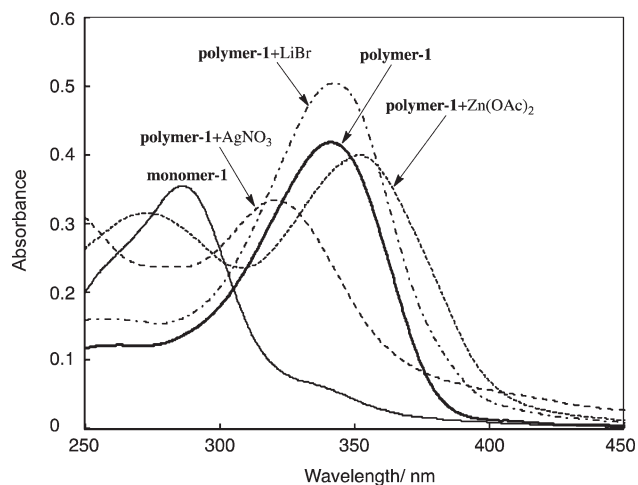
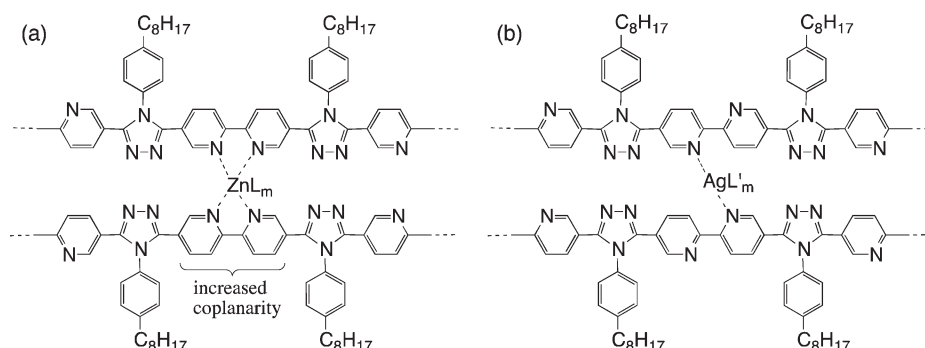


Figure 3. UV–vis spectra of the chloroform solutions of **monomer 1** and **polymer 1** ( $c = 1.0 \times 10^{-5} \text{ M}$ ) in the absence and presence of metal salts ( $[\text{metal salt}]/[\text{polymer 1}] = 30$ ).





**Chart 1.** Possible structures of polymer metal complexes.

reported study which shows that the PL intensities of  $\pi$ -conjugated polymers decrease with decreases in the distance between polymer chains in solution.<sup>22</sup> To confirm that the quenching and decrease of PL in **polymer 1** was because of the addition of  $\text{AgNO}_3$  and  $\text{Zn}(\text{OAc})_2$ , PL measurements of **polymer 1** in the presence of  $\text{AgNO}_3$  and  $\text{Zn}(\text{OAc})_2$  were conducted. The PL intensities decreased with an increase in the amounts of  $\text{AgNO}_3$  and  $\text{Zn}(\text{OAc})_2$ . A quantitative measurement of the PL quenching can be achieved by determining the Stern–Volmer constant,  $K_{\text{SV}}$ :

$$I_0/I = 1 + K_{\text{SV}} [\text{quencher}],$$

where  $I_0$  is the intensity of the PL in the absence of the quencher and  $I$  is the intensity of the PL in the presence of the quencher. The equation reveals that  $I_0/I$  increases in direct proportion to the concentration of the quenching moiety, and the constant  $K_{\text{SV}}$  defines the efficiency of quenching. Figure 5 shows Stern–Volmer plots for PL quenching by  $\text{AgNO}_3$  and  $\text{Zn}(\text{OAc})_2$  for **polymer 1**. The  $K_{\text{SV}}$  values of **polymer 1** when  $\text{AgNO}_3$  and  $\text{Zn}(\text{OAc})_2$  were used as quenchers were  $4.2 \times 10^7 \text{ M}^{-1}$  and  $1.1 \times 10^7 \text{ M}^{-1}$ , respectively. The  $K_{\text{SV}}$  value of **polymer 1** in the presence of  $\text{AgNO}_3$  was higher than that in the presence of  $\text{Zn}(\text{OAc})_2$ . This corresponds to the assumption that **polymer 1** formed a polymer complex with  $\text{AgNO}_3$  more easily than with  $\text{Zn}(\text{OAc})_2$ . This assumption is based on the abovementioned

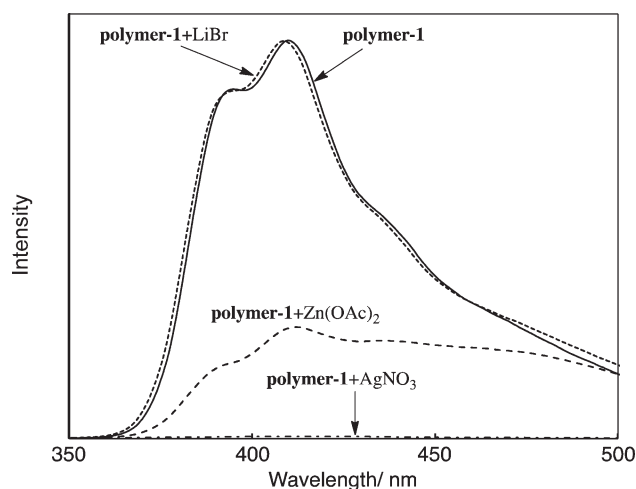
fact that  $\text{AgNO}_3$  and  $\text{Zn}(\text{OAc})_2$  coordinate with **polymer 1** to form the linear and regular tetrahedral complexes, respectively.

The quantum yield ( $\Phi$  value) of the chloroform solution of **polymer 1** was 0.21; this  $\Phi$  value was larger than that of the trifluoroacetic acid solution of **polymer 1** ( $\Phi = 0.19$ ). The low  $\Phi$  value of the trifluoroacetic acid solutions of **polymer 1** is apparently the result of the formation of the pyridinium salt with trifluoroacetic acid. It has been reported that pyridinium salts decrease the PL of photoluminescent  $\pi$ -conjugated polymers.<sup>23</sup>

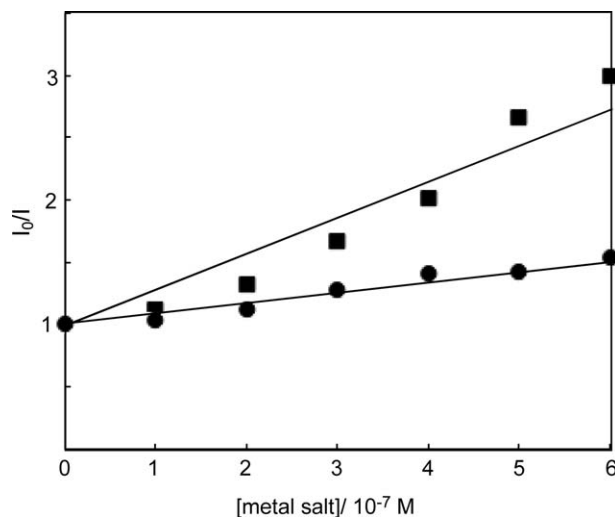
#### Cyclic Voltammograms

Figure 6 shows the cyclic voltammograms of the DMSO solution containing **monomer 1** and  $[\text{Et}_4\text{N}]\text{BF}_4$  (0.10M) and the cast film of **polymer 1** in a DMSO solution containing  $[\text{Et}_4\text{N}]\text{BF}_4$  (0.10M). Scheme 3 shows the electrochemical oxidation and reduction reactions of **polymer 1**.

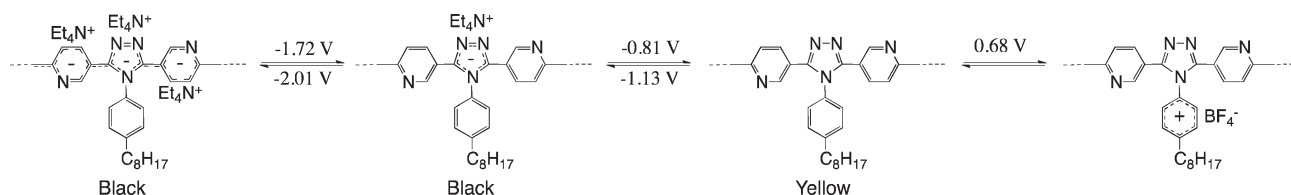
**Monomer 1** and **polymer 1** exhibited a peak at  $-2.19 \text{ V}$  ( $E_{\text{pc}}$  vs.  $\text{Ag}^+/\text{Ag}$ ) and  $-1.37 \text{ V}$  ( $E_{\text{pc}}$  vs.  $\text{Ag}^+/\text{Ag}$ ) and  $-2.01 \text{ V}$  ( $E_{\text{pc}}$  vs.  $\text{Ag}^+/\text{Ag}$ ) and  $-1.13 \text{ V}$  ( $E_{\text{pc}}$  vs.  $\text{Ag}^+/\text{Ag}$ ) corresponding to the electrochemical reduction of the pyridine and triazole rings, respectively. The observation that the reduction potentials of **polymer 1** is more positive than those of **monomer 1** corresponds to the longer  $\pi$ -conjugation length of **polymer 1** than **monomer 1**. The corresponding oxidation (n-dedoping) peaks



**Figure 4.** PL spectra of the chloroform solution of **polymer 1** in the absence and presence of metal salts.



**Figure 5.** Stern–Volmer plots for PL quenching by  $\text{AgNO}_3$  (square plots) and  $\text{Zn}(\text{OAc})_2$  (circle plots) for **polymer 1**.



**Scheme 3.** Electrochemical oxidation and reduction reactions of polymer 1.

of **polymer 1** were observed at  $-1.72$  V ( $E_{pa}$  vs.  $Ag^+/Ag$ ) and  $-0.81$  V ( $E_{pa}$  vs.  $Ag^+/Ag$ ), respectively. The yellow film of **polymer 1** changed to black after the electrochemical reduction and returned to yellow after crossing the  $E_{pa}$  peak. The high solubility of **polymer 1** in organic solvents may enable to prepare large area electrochromic devices with a simple cast film production method. **Monomer 1** and **polymer 1** exhibited a peak at  $0.65$  V ( $E_{pa}$  vs.  $Ag^+/Ag$ ) and  $0.68$  V ( $E_{pa}$  vs.  $Ag^+/Ag$ ) corresponding to the electrochemical oxidation of the octylphenyl group. Essentially the same  $E_{pa}$  values of **monomer 1** and **polymer 1** are attributed to the fact that the  $\pi$ -conjugation system of the polymer backbone is not expanded to the octylphenyl ring, because the octylphenyl ring is perpendicular to the triazole ring. Density functional theory calculations suggest that the benzene ring at the 4-position of 3,5-diphenyl-4-(4-hydroxyphenyl)triazole is perpendicular to the triazole ring.<sup>24</sup>

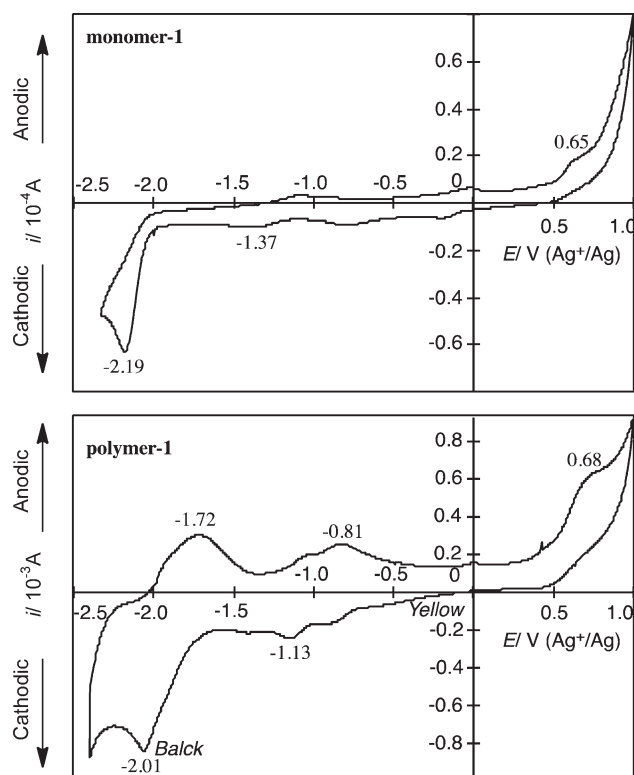


**Figure 6.** Cyclic voltammograms of (a) the DMSO solution containing **monomer 1** and  $[Et_4N]BF_4$  (0.10M) and a cast film of **polymer 1** in a DMSO solution containing  $[Et_4N]BF_4$  (0.10 M) (b). Swept rate was  $50$   $mV s^{-1}$ . The potential was scanned in the range of  $1.0$  V (vs.  $Ag^+/Ag$ ) to  $-2.3$  V (vs.  $Ag^+/Ag$ ) with a swept rate of  $50$   $mV s^{-1}$ .

### Electric Conductivity and Seebeck Coefficient

n-Doping of **polymer 1** was carried out by treating it with sodium naphthalenide in THF. The n-doped polymer exhibited electric conductivity ( $\sigma = 1.4 \times 10^{-5}$   $S cm^{-1}$ ) that was approximately  $10^2$  times higher than that of the respective non-doped polymer ( $\sigma = 2.2 \times 10^{-7}$   $S cm^{-1}$ ). The  $\sigma$  value of the n-doped polymer decreased to that of non-doped polymer when it was allowed to stand in air. This is because the reduced polymers are dedoped by oxidation in air.

Figure 7 shows temperature dependence of Seebeck coefficients ( $S$ 's) of **polymer 1** and **polymer-BiCl<sub>3</sub>** in the range of  $300$ – $360$  K. The negative  $S$  values of **polymer 1** and **polymer-BiCl<sub>3</sub>** suggest that the majority carrier of the polymers are electrons. This corresponds to the structures of **polymer 1** and **polymer-BiCl<sub>3</sub>**, which are composed of  $\pi$ -electron deficient aromatic rings. The absolute  $S$  values of **polymer 1** and **polymer-BiCl<sub>3</sub>** almost linearly increase with temperature. This behavior is consistent with the fact that Seebeck coefficients of conducting polymers usually increase almost linearly with temperature.<sup>25,26</sup> The  $S$  values of **polymer-BiCl<sub>3</sub>** are lower than those of **polymer 1** and can be attributed to the low  $S$  values of  $BiCl_3$  ( $S = -5.9$   $\mu V K^{-1}$  at  $310$  K and  $-5.6$   $\mu V K^{-1}$  at  $329$  K).

### CONCLUSIONS

A soluble n-type  $\pi$ -conjugated polymer (**polymer 1**) composed of a 1,2,4-triazole ring substituted by a 4-*n*-octylphenyl subunit at the 4-position of the 1,2,4-triazole ring and pyridine-2,5-diyl rings was synthesized by Ni(0)-complex-promoted dehalogenation polycondensation. The reaction of **polymer 1** with  $BiCl_3$  afforded a polymer–metal complex, **polymer-BiCl<sub>3</sub>**. The UV–vis

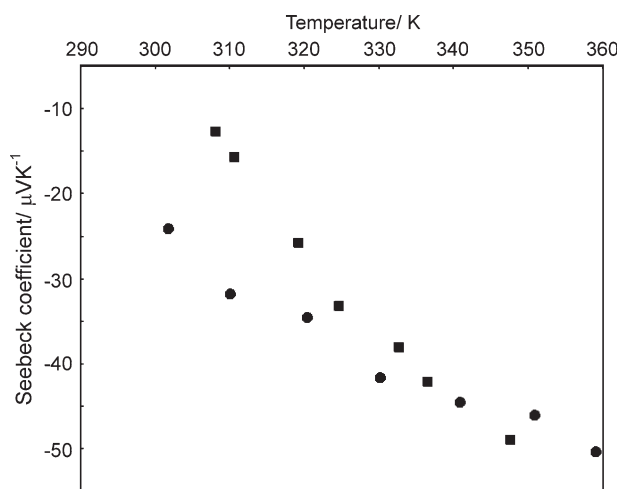


**Figure 7.** Temperature dependence of Seebeck coefficients of **polymer 1** (circle plots) and **polymer-BiCl<sub>3</sub>** (square plots).

measurements suggest that the  $\pi$ -conjugation system of the polymer is expanded along the polymer chain. The addition of metal salts to the **polymer 1** solution decreased the intensity of the PL peak with a shift of the PL peak. **Polymer 1** was electrochemically active in film, and the electrochemical reaction was electrochromic. Thermoelectric measurements of **polymer 1** and **polymer-BiCl<sub>3</sub>** suggest that their majority carriers are electrons. From the results obtained in this study, we concluded that metal complexation is effective for changing the optical and thermoelectric properties of n-type  $\pi$ -conjugated polymers.

## REFERENCES

1. List, E. J. W.; Scherf, U. In *Handbook of Conducting Polymers*, 3rd ed.; Skotheim, T.; Reynolds, J., Eds.; CRC Press: New York, **2007**.
2. Zahra, D.; Swagger, T. M. *J. Am. Chem. Soc.* **2009**, *131*, 17724.
3. Angulo, G.; Kapturkiewicz, A.; Palmaerts, A.; Lutsen, L.; Cleij, T. J.; Vanderzande, D. *Electrochim. Acta* **2009**, *54*, 1584.
4. Chai, J.; Wang, C.; Jia, L.; Pang, Y.; Graham, M.; Cheng, S. Z. D. *Synth. Met.* **2009**, *159*, 1443.
5. Brazen, A. L.; Mansfield, S. C. B.; Hamburger, P. J.; Ohuchi, F. S.; Boa, Z.; Janice, S. A.; Xiao, Y. *Chem. Mater.* **2008**, *20*, 4712.
6. Quits, P. A. C.; Swenson, J.; Ketoses, M. M.; Savernake, T. J.; Siebelles, L. D. A. *J. Phys. Chem. C* **2007**, *111*, 4452.
7. Zoo, Y.; Hour, J.; Yang, C.; Li, Y. *Macromolecules* **2006**, *39*, 8889.
8. Dubois, C. J.; Abound, K. A.; Reynolds, J. R. *J. Phys. Chem. B* **2004**, *108*, 8550.
9. Babel, A.; Janice, S. A. *J. Am. Chem. Soc.* **2003**, *125*, 13656.
10. Zhang, F.; Jonforsen, M.; Johansson, D. M.; Andersson, M. R.; Inganäs, O. *Synth. Met.* **2003**, *138*, 555.
11. Yamamoto, T.; Maruyama, T.; Zhou, Z. H.; Ito, T.; Fukuda, T.; Yoneda, Y.; Begum, F.; Ikeda, T.; Sasaki, S. *J. Am. Chem. Soc.* **1994**, *116*, 4832.
12. Maruyama, T.; Kubota, K.; Yamamoto, T. *Macromolecules* **1993**, *26*, 4055.
13. Yamaguchi, I.; Mitsuno, H. *Macromolecules* **2010**, *43*, 9348.
14. Yamaguchi, I.; Uehara, R. *Polym. Int.* **2013**, *62*, 766.
15. Bell, L. E. *Science* **2008**, *321*, 1457.
16. Du, Y.; Shen, S. Z.; Cai, K.; Casey, P. S. *Prog. Polym. Sci.* **2012**, *37*, 820.
17. Zhang, B.; Sun, J.; Katz, H. E.; Fang, F.; Opila, R. L. *ACS Appl. Mater. Int.* **2010**, *2*, 3170.
18. He, M.; Ge, J.; Lin, Z.; Feng, X.; Wang, X.; Lu, H.; Yanga, Y.; Qiu, F. *Energy Environ. Sci.* **2012**, *5*, 8351.
19. Tsai, L. R.; Chen, Y. *Macromolecules* **2007**, *40*, 2984.
20. Hightower, S.; Hard, M. *Chem. Mater.* **2004**, *16*, 3963.
21. Brown, D. J. *The Chemistry of Heterocyclic Compounds, Pyridine Metal Complexes*; Wiley: New York, **1985**, p 151.
22. Kim, J.; McQuade, D. T.; McHugh, S. K.; Swager, T. M. *Angew. Chem. Int. Ed.* **2000**, *39*, 3868.
23. Dwight, S. J.; Gaylord, B. S.; Hong, J. W.; Bazan, G. C. *J. Am. Chem. Soc.* **2004**, *126*, 16850.
24. Yamaguchi, I.; Mitsuno, H. *React. Funct. Polym.* **2011**, *71*, 140.
25. Masubuchi, S.; Kazama, S.; Mizoguchi, K.; Honda, M.; Kume, K.; Matsushita, R.; Matsuyama, T. *Synth. Met.* **1993**, *57*, 4962.
26. Kemp, T.; Kaiser, A. B.; Liu, C. J.; Chapman, B.; Mercier, O.; Carr, A. M.; Trodahl, H. J.; Buckley, R. G.; Partridge, A. C.; Lee, J. Y.; Kim, C. Y.; Bartl, A.; Dunsch, L.; Smith, W. T.; Shapiro, J. S. *J. Polym. Sci. Part B: Polym. Phys.* **1999**, *37*, 953.